Unconventional Methods for Geoscience, Shale Gas and Petroleum in the 21st Century
J. Watada et al. (Eds.)

doi:10.3233/AERD230007

The Impact of Contact Area and Fracture Surface Roughness on Fluid Flow in Fractured Reservoirs

Faisal Awad ALJUBOORI [a,1], Jang Hyun LEE [b] Khaled A. ELRAIES [b]
Karl D. STEPHEN [c]
[a] *North Oil Company, Ministry of Oil, Kirkuk 36001, Iraq*
[b] *Universiti Teknologi PETRONAS, 32610 Seri Iskandar, Perak Darul Ridzuan, Malaysia*
[c] *Institute of GeoEnergy Engineering, Heriot-Watt University, Edinburgh EH14 4AS, United Kingdom*
ORCiD ID: Faisal Awad ALJUBOORI https://orcid.org/0000-0002-3659-2744

Abstract.
The estimation of effective fracture permeability depends mainly on the geometry of the void space between the fracture surfaces. Sometimes, these void spaces are closed partially or totally for various reasons, which create a contact area between the fracture surfaces. These contact areas cause the fluid to follow a tortuous path around them, which reduces the permeability magnitude notably.

In this study, a digitised fracture network of a carbonate formation has been used to investigate the impact of contact areas and variable aperture width on the effective fracture permeability by using a discrete fracture networks approach. Moreover, a statistical analysis of a fracture width was used to build a stochastic aperture distribution to evaluate the fluid flow behaviour. Where, the properties of the aperture histogram are the only required parameters for the aperture modelling, in addition to several advantages in the current workflow compared with the former modelling approaches.

The results were represented by a correction curve plotted based on the 3D simulation results, which can be used to evaluate the reduction factor in fracture permeability by considering the impact of contact areas in fractures. Furthermore, it can also be utilised for the history-matching process by calibrating the fracture permeability, hence fluid flow behaviour at the well region or the reservoir scale.

Keywords. Fracture Surface Roughness, Fracture Aperture, Fracture Contact Area, Fracture Permeability, DFN Modelling

1. Introduction

Naturally fractured reservoirs are highly heterogeneous systems, where fractures control the reservoir permeability, and hence the fluid flow behaviour [1,2,3,4]. Therefore, accurate modelling of the fracture network has a key role in the development of such

[1] Corresponding Author: ALJUBOORI Faisal Awad, f.a.aljuboori@gmail.com

complicated reservoirs [5,6,7]. Moreover, the estimation of fracture permeability is a challenging task. The variability in the fracture width, which is difficult to predict, has a major impact on fracture permeability. Several approaches have been suggested to predict the variability in the fracture width by creating fracture surfaces using Gaussian and Self-Affine autocorrelations (e.g. [8,9,10,11]).

Furthermore, Adler et al. [11] have detailed the required statistical analysis parameters (such as; surface roughness (σ_h), surface fluctuation ($h^{\pm}$), correlation length (l_c), … etc.) to describe the random fracture properties and to build fracture surfaces. Although it is important to understand the fluid flow and the role of each parameter in a small-scale model, a more practical approach is necessary for sector or full-field modelling. The effect of some of the previously mentioned parameters such as; surface roughness (σ_h), is an apparent reduction factor used to correct the deviation from the ideal parallel plate concept which has been assumed in the derivation of the cubic law [10,12]. Therefore, the overall formula can be adjusted by considering a factor (f) which was found to be varied from (1.04 – 1.65) [10].

Nevertheless, the suggested detailed description of creating fracture surfaces is applicable for 2D models of Finite Element modelling (e.g. [11,13,14,15]), whilst it would be impossible to apply the same procedure for hundreds to thousands of 3D fractures in a full field modelling. Moreover, the 2D models cannot represent the natural fracture connectivity because the non-connecting fracture in the planer view may be connected in the third dimension [10]. Therefore, proposing a convenient approach is necessary to model the fracture properties at a large-scale (*sector or full field*), without neglecting the small-scale heterogeneity of the fracture surfaces such as roughness and contact area.

In this paper, both roughness and contact area were represented in the modelling by generating fracture apertures property using their frequency distribution data provided by Bisdom et al. [15]. The statistical properties of the fracture aperture histogram have been used as the input data for *Sequential Gaussian Simulation* (*SGS*) distribution. Furthermore, considering the geological description and core examination (*if the core data are sufficient and representative*) could improve the distribution. The fracture permeability was estimated using the parallel plate law (*cubic law*), as illustrated in **Equation 1**. However, detailed mathematical descriptions can be found in several references (e.g. [10,11,12]).

$$Fracture\ Permeability\ (m^2) = \frac{Aperture\ (m)^2}{12} \tag{1}$$

The key difference in this work is that we evaluate the fracture contact area effect in 3D models with variable aperture. In addition, the advantage of the proposed methodology includes; *scale flexibility*, *fewer parameters required for modelling*, *the ability to consider the matrix contribution to the fracture performance*, and *an improved understanding of the differences in the fluid flow pattern*.

It is worth mentioning that outcrop studies provide valuable information about the fracture characteristics and their properties, which can be used as effective input data for fracture modelling [3,16,17,18].

2. Geological Description of the Fracture Network

The studied outcrop area is located in central Tunisia, in the foothills of the Tunisian Atlas in the Gafsa Basin, see **Figure 1**. An excellent outcrop exposure of fractured Eocene Carbonate of Kef Eddour Formation has been utilised to extract the fracture network using Unmanned Aerial Vehicle (*UAV* or "*drone*"). The acquired orthophotos have accurately been processed to extract a fracture dataset [19,20], as shown in **Figure 2**. Additional details about this outcrop, analysis of the digitised fracture sets could be found in [19]. Meanwhile, the acquired and processed outcrop images could be found in [20].

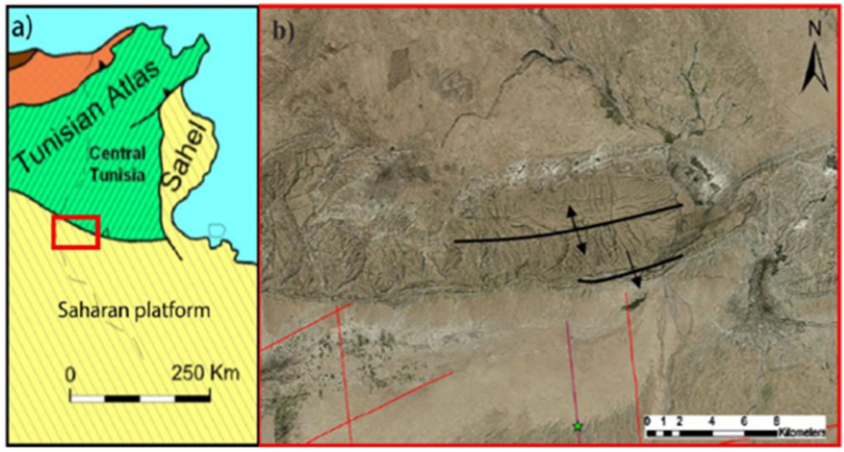

Figure 1. The outcrop location (a) Gafsa basin setting (b) Enlargement of the red box area in (a) showing the Alima anticline in the centre. The red lines represent the top of the seismic sections. the green star indicates a well, after Bisdom et al. [19]

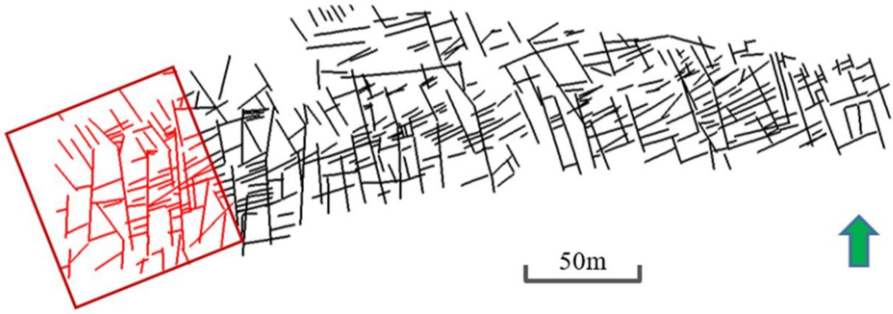

Figure 2. The digitised fracture network from the outcrop, the highlighted part of the network (indicated by red colour) has been utilised in the current workflow, after Aljuboori et al. [21].

The processed and interpreted outcrop images can be used in fracture modelling [22]. The digitised fractures may be preserved in the reservoir simulation model (i.e, to be modelled deterministically) [23].

3. Modelling Workflow Steps

A systematic workflow was suggested to estimate the reduction in system permeability due to various reasons (e.g., *diagenesis alteration*, *cementation*, *field stress changes*, ... *etc.*). The workflow starts after the fractures were upscaled to the grid. At this step, both fracture aperture and permeability were not defined yet. The aperture distribution, which has been used to assign the value of the fracture aperture, could be extracted from *outcrop studies*, *FMI interpretation* or *geomechanical modelling results*. The proposed workflow has been summarised in the following steps: -

1. Modelling the fractures deterministically or stochastically. An example of deterministic fracture modelling has been illustrated in **Figure 3** below:

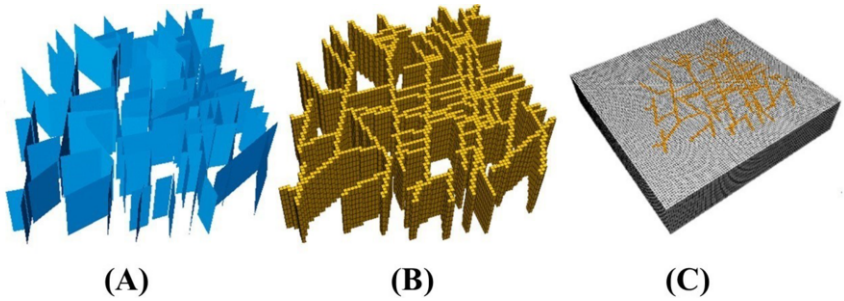

Figure 3. Example of deterministic fracture modelling, (A) Digitised fracture network (B) The corresponding fractured cells in the model (C) Flow simulation model showing the fractures (yellow cells) and the matrix (grey cells)

2. Populate the fractures with aperture property using Sequential Gaussian Simulation (SGS) and aperture distribution properties as input data (such as; *minimum* and *maximum aperture width*, *mean* and *standard deviation*), see **Figure 4**. Then, calculate the fracture permeability using the cubic law, as given in **Equation 1**.

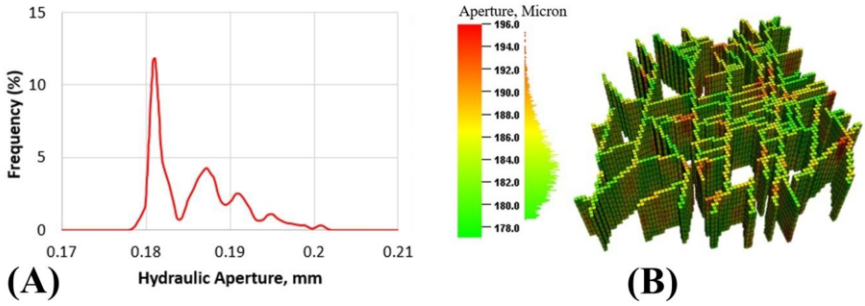

Figure 4. (A) Aperture distribution histogram, (B) Populated fractured cells in the grid with aperture values based on aperture distribution

3. Run the model by defining a single producer located at the grid centre and interpret the system permeability (k_a) using the well test technique, i.e. system permeability when all the fractures are fully open to the fluid flow (Zero contact area - *Base Case scenario*).

4. Assign zero aperture values to the smallest apertures based on the illustrated distribution in **Figure 4**. The aperture values have already been populated in step (2) as a property. Then, if we aim, for example, to close any aperture below (0.178 mm) of the distribution, as illustrated in **Figure 5** labelled by the first selection. A simple conditional "if" formula could be used in the software calculator to shut these apertures totally as follows: -

$$New\ Aperture = if(Aperture \leq 0.178\ ,\ 0\ ,\ Aperture) \tag{2}$$

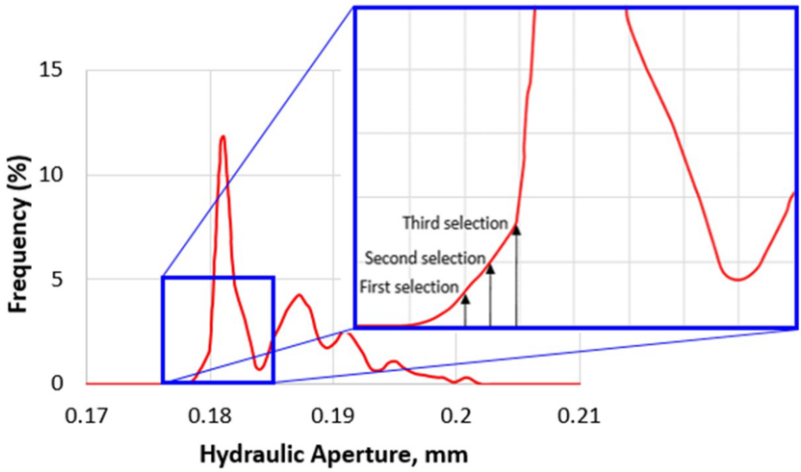

Figure 5. Aperture distribution histogram, the blue box is showing an example of how to choose the smallest apertures and close them gradually.

At this step, the number of zero aperture cells has been determined, and the percentage of the contacted area is calculated. The well test procedure has been used to determine the permeability. The interpreted permeability at this step should be less than the permeability value determined in step (3) due to the effect of zero aperture (contacted area cells).

5. Repeat step (4) for the next range (labelled by second selection in **Figure 5**) of the aperture to be closed and determined the system permeability.
6. Repeat step (5) until the contacted area reached 30% or more as required.
7. Plot the normalised permeability (k/k_a) versus the percentage of the contacted area to conclude the permeability reduction curve.

The above steps could be applied to any fracture network to estimate the reduction in fracture permeability due to the sealed aperture by cementation or any other reasons, which should be supported by outcrop or sedimentology studies. Moreover, the same procedure has been applied to the 2D models and 3D single aperture models except for step (2), where a single value of aperture was assigned. In addition to using *Sequential Indicator Simulation* (SIS) or *Truncated Gaussian Simulation* (TGS) approaches to distribute the zero aperture cells randomly.

4. Setup of Numerical Simulation Models

4.1. 2D Simulation Models

Fine-scale 2D models in the XY-direction were generated based on a horizontal fracture extended for (100 m) in both directions, and (0.3 mm) in the Z direction, which represents the fracture aperture dimension. This fracture has been upscaled to the 2D grid, which has the dimension of (100m×100m×0.5m), with (1m×1m×0.5m) resolution as shown in **Figure 6(A)**. The initial mechanical aperture has assumed to be (0.3 mm) [15,24]. Furthermore, Barton et. al. [24] have explained that the initial mechanical aperture is a function of surface roughness only, as explained in **Equation 2**;

$$A_0 = \frac{JRC}{5}(0.2\,\frac{\sigma_c}{JCS} - 0.1) \tag{3}$$

Where;

A_0 *Initial mechanical aperture.*
JRC *Joint roughness coefficient.*
σ_c *Uniaxial compressive strength.*
JCS *Joint compressive strength.*

Further calculation details have been explained in [15,24]. The initial aperture of (0.3mm) was used to assign the fracture permeability in the grid by using the cubic law, see **Equation 1**, [12,21,25]. In addition, the real fluid properties of a carbonate reservoir have been adapted to initialise the model. The simulation scenarios of a grid's central producer have been organised into two groups; the first group scenario was based on a uniform distribution of the asperities (contact surfaces cells), **Figure 6(B)**. However, the second group scenario represents the asperities cells by random distribution, **Figure 6(C)**.

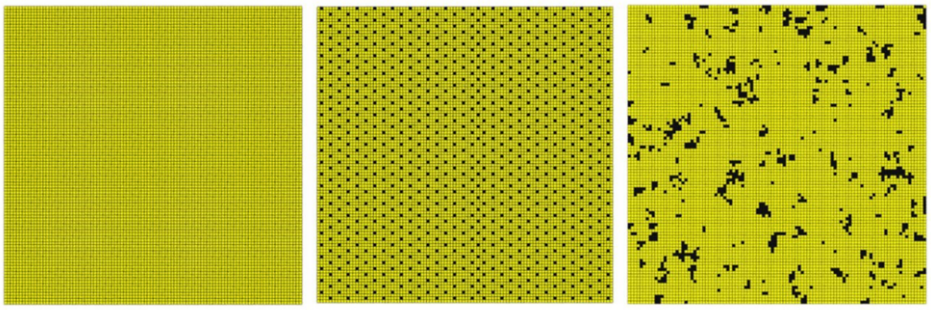

Figure 6. (A) 2D model with 0% of contact area, (B) Example of uniformly distributed 8% of the contact area (black cells), (C) Example of randomly distributed 8% of the contact area (black cells).

4.2. 3D Simulation Models

The illustrated fracture pattern in **Figure 2** (*the red part*), was imported into a geological modelling package and a fracture network was created deterministically in the model. The discrete fracture networks (DFN) approach was used, which is appropriate for well scale or sector modelling [5,6,26,27,28,29]. This work aims to investigate the effect of contact areas and fracture surface roughness on effective fracture permeability. Therefore, the matrix properties were set to zero, which helps to focus on the analysis of the fracture network response alone.

The shown flow simulation model in **Figure 3(C)** has based on the digitised fracture network of Kef Eddour Formation, see **Figure 3(A)**. The flow model has discretised into (100×100×8) grid cells (i.e., 80,000 grid cells in total), and it has dimensions of (100m×100m×4m). Fractures were assumed to be vertical in the model (dip 90° as observed in the outcrop) and an average aperture of (0.3 mm) [15]. Furthermore,the cubic law was employed to calculate the fracture permeability. The fluid properties of a carbonate reservoir were utilised to initialise the flow model to ensure realistic reservoir conditions and fluid composition. The fracture network honoured the detailed geological observations of the outcrop [30], see **Figure 3(B)**.

The increment of the contact area has been assessed by assuming an increasing range from (0 to 30%). The effective permeability of the fracture network has been calculated for each level of the contact area using the well test analysis (*the derivative and semi-log methods*) to analyse the simulation results. An example of The contact area is indicated by black cells in the model, as illustrated in **Figure 7**.

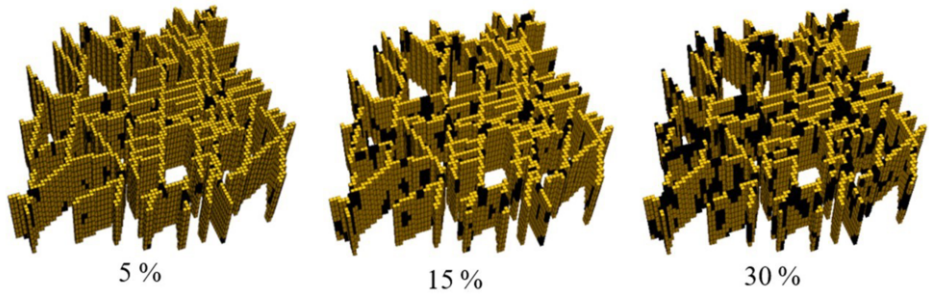

Figure 7. Fractured cells in the model, black cells represent the contact area with a closed aperture, where their proportion increased from 5% to 30%, and the yellow cells represent the open aperture.

The distribution of the black cells in the flow model can be generated using Sequential Indicator Simulation (SIS) or Truncated Gaussian Simulation (TGS) method. The seed number of the distribution has been fixed during the process to ensure that the previously assigned black cells remain in their locations while adding new black cells when the percentage of the contact area increased. The horizontal anisotropy range is 3 metres in both major and minor directions while the vertical range is 2 metres to mimic the heterogeneity of the fracture surface, and they are suitable to produce a smooth variation in the aperture distribution based on cell thickness.

All simulation scenarios have been carried out using the black oil simulator. The pressure drop in all scenarios was designed to maintain the grid pressure above the bubble point pressure to prevent any two-phase flow occurs during the flow period.

4.3. Gaussian Aperture Distribution Models

The fracture width (aperture) is the dominant parameter in estimating fracture permeability. However, in most fracture modelling workflow an average single value has been used for the estimation of fracture permeability or conductivity (e.g., [15,31,32,33,34]). Nevertheless, an alternative approach has been based on creating two fracture surfaces using the Gaussian or Self-affine method (e.g., [9,10,11]). The result of this approach is creating spaces with variable widths between the generated fracture surfaces, which represent the fracture aperture.

In the current work, the surface roughness of the fracture was investigated implicitly by assigning variable aperture. A statistical analysis of hydraulic fractures of the Kef Eddour formation, which has been presented in [15], was used in fracture permeability estimation. The hydraulic aperture frequency has been regenerated, as shown in **Figure 8 (A)**, to calculate their statistical properties such as mean, standard deviation, minimum and maximum aperture to be used in aperture distribution, **Figure 9 (A, B)** . The sequential Gaussian simulation was employed to obtain smooth changes in aperture distribution. A variable seed number was applied to generate multiple realizations using the same mean, standard deviation and correlation length. Moreover, the fracture permeability was calculated using the parallel plate law (the cubic law).

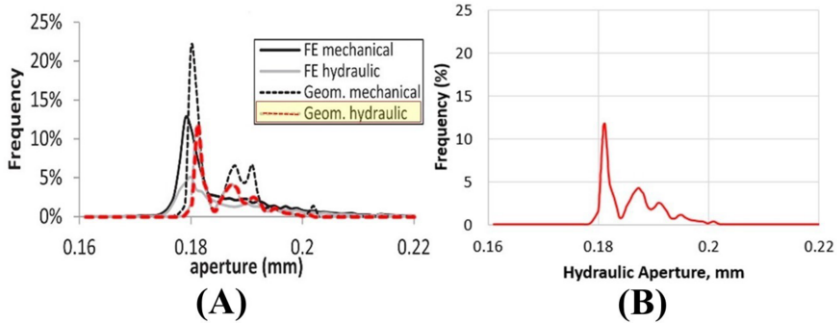

Figure 8. (A) Statistical frequency curve of hydraulic fracture of Kef Eddour formation (*the highlighted curve has been used in the aperture distribution*) (B) Re-generated statistical frequency of opening width (after the author permission [15]).

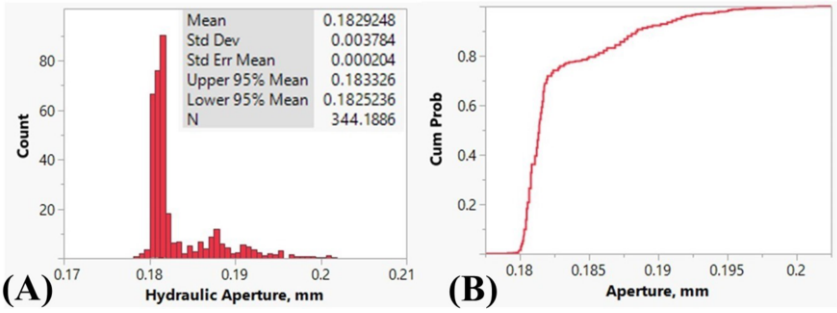

Figure 9. (A) Histogram of hydraulic aperture (B) Cumulative density function (CDF) plot.

5. Results

The results were divided into two parts, the first part summarises the 2D modelling that aimed to validate the proposed procedure of the current work (i.e., using a black oil simulator and well test analysis to assess the boundary element analysis method). In addition, carry out the 3D modelling of the contact surface effect and determine how the results may differ from 2D especially when using an outcrop fracture network compared to a single fracture generated stochastically using the Gaussian or self-affine approach. Whilst, the second part includes using real statistics of the aperture distribution, illustrated in **Figure 9**, as input data for 3D modelling via the Gaussian distribution. **Table 1** has summarised the total number of runs for each model: -

Table 1. Summary of the Simulation Runs

Model	2D Uniform	2D Random	3D Single Aperture value	3D Variable Aperture value
No of Runs	10	12	50	55

5.1. Results of 2D Models and 3D Single Aperture Models

The aim of the 2D models work is to validate the used approach of numerical simulation and the techniques of well test analysis, see **Figure 10**. A uniform distribution of the contact surfaces in the fractured grid was used with varying contact areas. The 2D simulation results produced an excellent match with the simulation results of Zimmerman et al. [8], as shown in **Figure 11**. Furthermore, The calculated shape factor from the 2D results is almost identical to the values obtained by Zimmerman et al. [8] which is around (1.5). However, the calculated normalized permeability of the 3D models has shown significantly lower values than the 2D models. Moreover, the calculated shape factor of the 3D simulation is completely different and generally higher than the 2D value, see **Figure 11**. The shape factor was calculated using the suggested formula by Zimmerman et al. [8] in the following **Equation 4**.

$$\frac{k}{k_a} = \frac{(1-\beta C)}{(1+\beta C)} \tag{4}$$

where;

k Fracture network permeability affected by contact area.
k_a Fracture network permeability when contact area is zero.
β Shape factor of the asperities
C Contact area percentage

Using the normalized permeability (k/k_a) allows comparing variable system permeabilities on the same basis. Furthermore, the mentioned 3D behaviour represents the fracture network performance only and the matrix has no contribution. Therefore, the effect of contact surfaces on fluid flow in 3D fracture network might be different in the case of matrix contribution, where the matrix permeability constitutes a bypass fluid path to the sealed fractures.

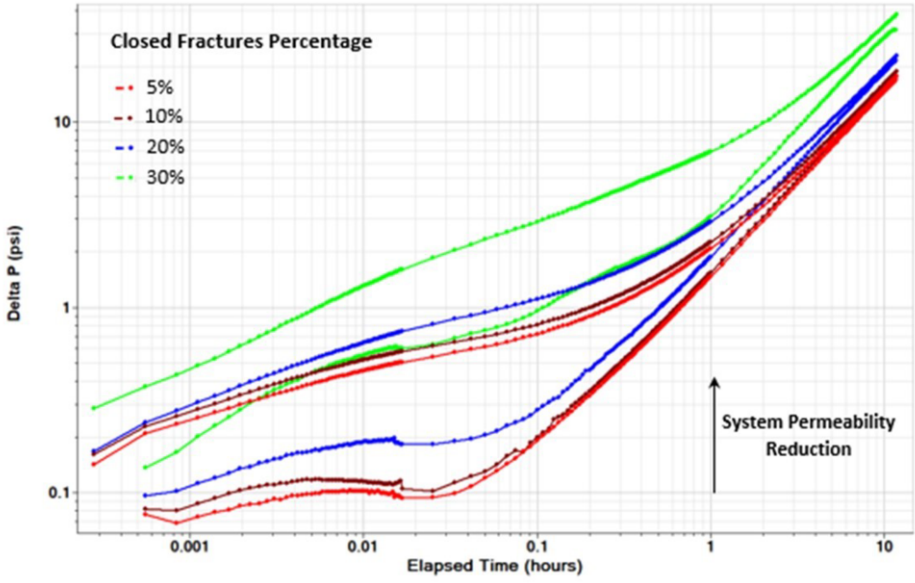

Figure 10. Example of pressure and pressure derivative response at various percentage of closed fractures.

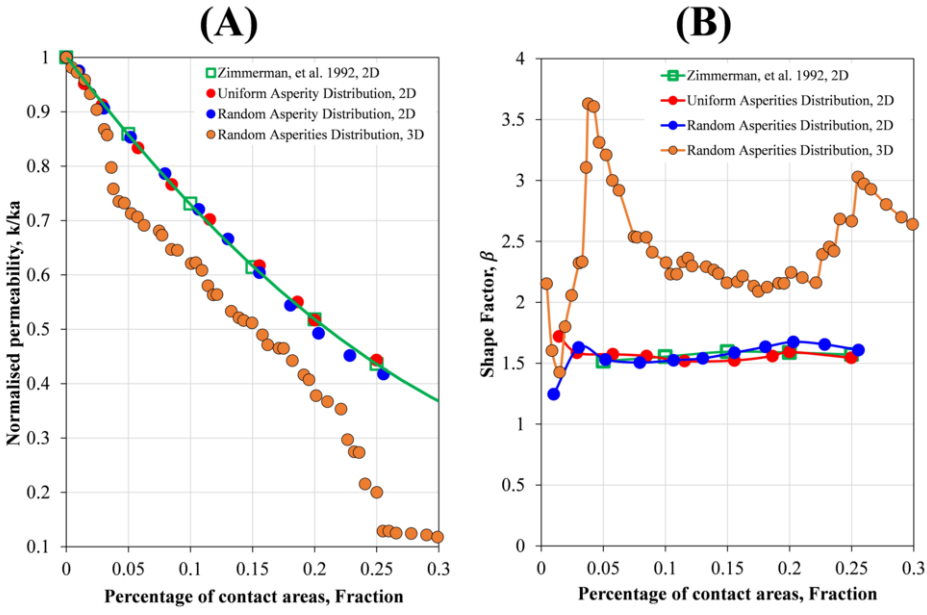

Figure 11. (A) Normalised permeability of the 2D models of the current work compared with the results of the presented 2D model by Zimmerman et al. [8] using the boundary element method. In addition, the result of the 3D has been included for comparison purposes, (B) comparison of the calculated shape factor for both 2D and 3D models.

5.2. Gaussian Aperture Distribution Model Results

Five realizations were generated to investigate the possible changes in the fracture permeability value due to contact surfaces. The results were shown insignificant changes in permeability (5.5%) for $\leq 5\%$ of contact cells, see **Figure 12**. However, it became significant and the permeability value reduced by (23%) for 13% of contact cells, nevertheless the permeability remains higher than predicted by 2D or 3D single aperture models. Finally, for more than 13% contact cells scattered results were obtained with a high range of permeability reduction, **Figure 12**. The results highlighted that the spatial distribution of contact areas and their clustering in the system can change the performance of the fluid flow dramatically.

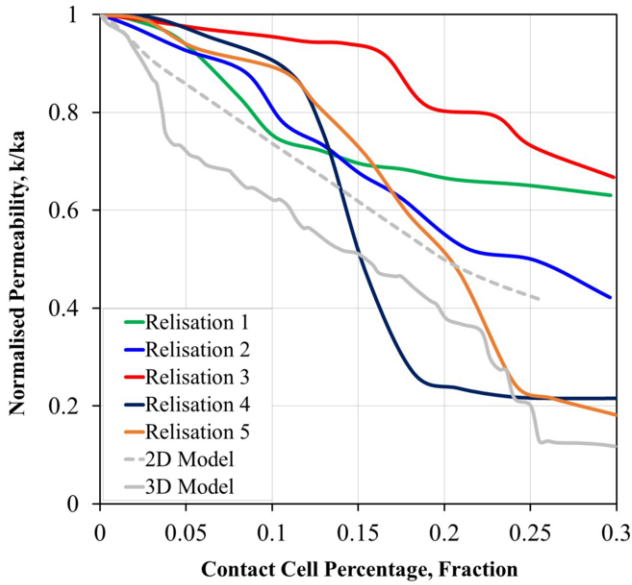

Figure 12. Normalised permeability of five realisations corresponds to the contact cell percentage in addition to the 2D and 3D results.

The growth in fracture contact area (represented by increasing cell percentage in the simulation model) has distributed via the Gaussian method and it was based on closing the smaller aperture in the illustrated histogram in **Figure 5** increasingly, which is more realistic to what happens in nature by precipitation, cementation or reservoir depletion.

6. Discussion

The 2D models (Uniform and Random distribution of the contact areas) produce very similar results regardless of their distribution mode. Whilst, the 3D single aperture models have shown a consistent and greater reduction in permeability when the percentage of the contact areas increased. This model has predicted a higher permeability reduction than 2D models.

In contrast, in the 3D variable aperture models, which considered the surface roughness implicitly through the variable aperture, the reduction in permeability is not as high as observed in the 3D single aperture models, where the impact is low until 13 % of contact areas.

The current work highlighted the importance of using real aperture distributions, as presented by several authors (e.g., [15,35]). The proposed workflow can be adapted to enhance the aperture distribution in fracture modelling, which is a critical parameter for the development of fractured reservoirs. Furthermore, the results of the 3D models have shown that the effect of contact surfaces or fracture roughness cannot be represented by a simple equation, and it is controlled by many factors such as matrix contribution and aperture distribution.

In summary, the current methodology of estimating the reduction in fracture permeability due to closed apertures could be employed to improve the history matching process by adjusting the fracture permeability or to simulate the fluid flow behaviour in a producer when the fractures in the simulation model over-performed. Where the fracture permeability could be used as a calibrating parameter [17,36]. Moreover, the following **Table 2** summarises the key differences between the current methodology and the previous approaches.

Table 2. Comparison table between the current methodology and the previous approaches

Items	Current work	Adler, et al. [11]	Zimmerman, et al. [8]
Scale	Flexible based on cell size "modeller choice"	No scale mentioned	No scale was mentioned, the used model was 30*30 grid cells
Dimension	2D and 3D models	2D model	2D model
Matrix effect	Can be included	Cannot be included	Cannot be included
Fluid flow pattern	Redial flow (similar to the flow in the reservoir to the wellbore)	Not mentioned	Linear flow from one end of the model to the other end cells
Required parameters for aperture modelling	Either Aperture (for single aperture value models) Or, Aperture histogram properties (for variable aperture value models)	1. The probability density, $\phi(h^{\pm})$. 2. Organisation of each surface by introducing an autocorrelation function. 3. The interrelation between the two fracture surfaces.	Aperture (single value)
Surface roughness	Included (implicitly in the 3D models only)	Included as a direct parameter	Not included
Aperture	Single and variable	variable	Single value
Assigning contact area	Through SIS or TGS based on aperture distribution and using the software calculator	Automatically, when the fracture surfaces are generated the overlap area is the contact area	Using the decay exponent of spatial correlation and damping factor
Permeability reduction	Estimated (2D and 3D models)	Not estimated	Estimated (2D models only)

7. Conclusions

It has been shown that the single-value assumption of fracture aperture may result in an inaccurate estimation of fluid flow performance in fractures. Furthermore, the fluid flow behaviour in the simple 2D models or 3D single aperture models can be misleading due to simple assumptions of fracture morphology. Whilst, the 3D variable aperture models have shown various fluid flow behaviour in fractures that might be obtained due to the spatial distribution of the closed apertures and their clustering under multiple distribution trials and different percentages of the contact surface. This variety of flow behaviour explains the complexity of the fracture network and its connectivity.

Although the distribution of the fracture aperture depends on the statistical analysis such as; *minimum and maximum aperture value*, *standard deviation*, and *mean* is not unique, it can help to understand the complexity of the subsurface aperture morphology and their impact through the range of results (i.e., realisations) that represents the uncertainties due to distribution. These results can be adapted in the risk analysis of the evaluation project and ranking of the parameters' impact on the fluid flow in fractures.

Moreover, the aperture distribution can be improved by defining its value as a continuous property at each well location (using core data or FMI interpretation). In addition, concluding a relationship between the fractures' aperture and a second property or parameter such as facies (especially dolomite) can be very helpful, where the second parameter can be used as a bivariate property in the distribution (i.e., improving the modelling workflow of the property).

The proposed workflow can be adapted to tune the fracture permeability in the history-matching process to avoid using global multipliers without justified reasons. The methodology of the current work has been based on using static conditions without considering the matrix effect, or aperture changes under dynamic conditions such as effective stress changes due to the reduction in the reservoir pressure during depletion. This process may lead to rock expansion and hence reduction in the fracture aperture, which reduces the effectiveness of fractures as a major fluid flow path in the reservoir.

8. Future work

The current work can be extended to consider the impact of several essential factors on the fluid flow behaviour in fractures, such as evaluating;

1. Matrix effect on the fracture performance, where the matrix permeability constitutes a flow path to bypass the closed fractures using a full-field model. It should be highlighted that this proposed work has been applied to a small-scale model by Aljuboori et al. [4], which can be used as a guide.
2. The change in the effective stress, and hence the fractures aperture, due to reservoir depletion or water injection.

References

[1] Faisal Awad Aljuboori, Jang Hyun Lee, Khaled A. Elraies, and Karl D. Stephen. The effectiveness of low salinity waterflooding in naturally fractured reservoirs. *Journal of Petroleum Science and Engineering*, 191:107167, 2020.

[2] Faisal Awad Aljuboori, Jang Hyun Lee, Khaled A. Elraies, Karl D. Stephen, and Muhammed Khan Memon. Modelling the transient effect in naturally fractured reservoirs. *Journal of Petroleum Exploration and Production Technology*, Feb 2022.

[3] Richard O. Baker and Frank Kuppe. *SPE-63286-MS*, chapter Reservoir Characterization for Naturally Fractured Reservoirs, page 11. Society of Petroleum Engineers, Dallas, Texas, 2000.

[4] Faisal Awad Aljuboori, Jang Hyun Lee, Khaled A. Elraies, and Karl D. Stephen. The impact of diagenesis precipitation on fracture permeability in naturally fractured carbonate reservoirs. *Carbonates and Evaporites*, 36(1):6, Nov 2020.

[5] B D M Gauthier, A M Zellou, A Toublanc, M Garcia, and J M Daniel. Integrated Fractured Reservoir Characterization: a Case Study in a North Africa Field. In *SPE-65118-MS*. Society of Petroleum Engineers, 2000.

[6] B D M Gauthier, M Garcia, and J M Daniel. Integrated Fractured Reservoir Characterization: A Case Study in a North Africa Field. *SPE-79105-PA*, 2002.

[7] Luis Guerreiro, Antonio Costa Silva, Victor Alcobia, and Amilcar Soares. Integrated Reservoir Characterisation of a Fractured Carbonate Reservoir. In *SPE-58995-MS*. Society of Petroleum Engineers, 2000.

[8] Robert W. Zimmerman, Di-Wen Chen, and Neville G.W. Cook. The effect of contact area on the permeability of fractures. *Journal of Hydrology*, 139(1):79–96, 1992.

[9] V.V. Mourzenko, J.-F. Thovert, and P.M. Adler. Permeability of a single fracture; validity of the reynolds equation. *J. Phys. II France*, 5(3):465–482, 1995.

[10] Muhammad Sahimi. *Flow and transport in porous media and fractured rock: from classical methods to modern approaches*. John Wiley & Sons, 2011.

[11] Pierre M. Adler, Jean-François Thovert, and Valeri V. Mourzenko. *Fractured Porous Media*. Oxford University Press, 10 2012.

[12] Paul Adams Witherspoon, Joseph SY Wang, K Iwai, and John E Gale. Validity of cubic law for fluid flow in a deformable rock fracture. *Water resources research*, 16(6):1016–1024, 1980.

[13] P C Robinson. Connectivity of fracture systems-a percolation theory approach. *Journal of Physics A: Mathematical and General*, 16(3):605, feb 1983.

[14] P C Robinson. Numerical calculations of critical densities for lines and planes. *Journal of Physics A: Mathematical and General*, 17(14):2823, oct 1984.

[15] Kevin Bisdom, Giovanni Bertotti, and Hamidreza M Nick. A geometrically based method for predicting stress-induced fracture aperture and flow in discrete fracture networks. *AAPG Bulletin*, 100(7):1075–1097, 2016.

[16] C.L. Jensen, S.H. Lee, W.J. Milliken, J. Kamath, W. Narr, H. Wu, and J.P. Davies. Field simulation of naturally fractured reservoirs using effective permeabilities derived from realistic fracture characterization. SPE Annual Technical Conference and Exhibition, 09 1998. SPE-48999-MS.

[17] J. C. Sabathier, B. J. Bourbiaux, M. C. Cacas, and S. Sarda. *SPE-39825-MS*, chapter A New Approach of Fractured Reservoirs, page 11. Society of Petroleum Engineers, Villahermosa, Mexico, 1998.

[18] Ben J. Stephenson, Anton Koopman, Heiko Hillgartner, Harry McQuillan, Stephen Bourne, Jon J. Noad, and Keith Rawnsley. Structural and stratigraphic controls on fold-related fracturing in the zagros mountains, iran: implications for reservoir development. *Geological Society, London, Special Publications*, 270(1):1–21, 2007.

[19] K. Bisdom, G. Bertotti, and B.D.M. Gauthier. Predicting multi-scale deformation and fluid flow patterns in folds using 3d outcrop models and mechanical modelling. Number 1, pages 1–5. European Association of Geoscientists and Engineers, 2014.

[20] Kevin Bisdom. Natural fracture patterns in carbonate rocks, 2015.

[21] Faisal Aljuboori, Patrick Corbett, Kevin Bisdom, Giovanni Bertotti, Sebastian Geiger, Kevin Bisdom, and Giovanni Bertotti. Using Outcrop Data for Geological Well Test Modelling in Fractured Reservoirs. Number June 2015, pages 1–4, Madrid, Spain, 1-4 June, 2015.

[22] B. J. Bourbiaux, M. C. Cacas, S. Sarda, and J. C. Sabathier. *SPE-38907-MS*, chapter A Fast and Efficient Methodology to Convert Fractured Reservoir Images Into a Dual-Porosity Model, page 12. Society of Petroleum Engineers, San Antonio, Texas, 1997.

[23] Patrick WM Corbett, Sebastian Geiger-Boschung, Lindemberg Pinheiro Borges, Mikayil Garayev, Julio Gabriel Gonzalez, Camilo Valdez, et al. Limitations in numerical well test modelling of fractured carbonate rocks. In *SPE EUROPEC/EAGE Annual Conference and Exhibition*. Society of Petroleum Engineers, 2010.

[24] N. Barton, S. Bandis, and K. Bakhtar. Strength, deformation and conductivity coupling of rock joints. *International Journal of Rock Mechanics and Mining Sciences & Geomechanics Abstracts*, 22(3):121–140, 1985.

[25] Sebastian Geiger and Stephan Matthäi. What can we learn from high-resolution numerical simulations of single- and multi-phase fluid flow in fractured outcrop analogues? *Geological Society, London, Special Publications*, 374(1):125–144, 2014.

[26] William S. Dershowitz, J Hermanson, S Follin, and M Mauldon. Fracture intensity measures in 1-D, 2-D, and 3-D at Aspo, Sweden. *Pacific Rocks 2000: Rock around the Rim*, 2000.

[27] Bill Dershowitz, Paul LaPointe, Thorsten Eiben, and Lingli Wei. Integration of Discrete Feature Network Methods With Conventional Simulator Approaches. *SPE Reservoir Evaluation & Engineering*, 3(02):165–170, 04 2000.

[28] Bernard Bourbiaux, Rémy Basquet, Marie-Christine Cacas, Jean-Marc Daniel, and Sylvain Sarda. An Integrated Workflow to Account for Multi-Scale Fractures in Reservoir Simulation Models: Implementation and Benefits. volume All Days of *Abu Dhabi International Petroleum Exhibition and Conference*, 10 2002. SPE-78489-MS.

[29] H. Kazemi, S. Atan, M. Al-Matrook, J. Dreier, and E. Ozkan. Multilevel Fracture Network Modeling of Naturally Fractured Reservoirs. volume All Days of *SPE Reservoir Simulation Conference*, 01 2005. SPE-93053-MS.

[30] Simeon Agada, Sebastian Geiger, and Florian Doster. Wettability, hysteresis and fracture–matrix interaction during co2 eor and storage in fractured carbonate reservoirs. *International Journal of Greenhouse Gas Control*, 46:57–75, 2016.

[31] L. Cosentino, Y. Coury, J. M. Daniel, E. Manceau, C. Ravenne, P. Van Lingen, J. Cole, and M. Sengul. Integrated Study of a Fractured Middle East Reservoir with Stratiform Super-K Intervals – Part 2: Upscaling and Dual Media Simulation. volume All Days of *SPE Middle East Oil and Gas Show and Conference*, 03 2001. SPE-68184-MS.

[32] Zeno G. Philip, Jr. Jennings, James W., Jon E. Olson, and Jon Holder. Modeling Coupled Fracture-Matrix Fluid Flow in Geomechanically Simulated Fracture Networks. volume All Days of *SPE Annual Technical Conference and Exhibition*, 09 2002. SPE-77340-MS.

[33] Sandra Jenni, Lin Y. Hu, Rémy Basquet, Ghislain de Marsily, and Bernard Bourbiaux. History Matching of Stochastic Models of Field-Scale Fractures: Methodology and Case Study. SPE Annual Technical Conference and Exhibition, 09 2004. SPE-90020-MS.

[34] Arnaud van Harmelen and Ruud Weijermars. Complex analytical solutions for flow in hydraulically fractured hydrocarbon reservoirs with and without natural fractures. *Applied Mathematical Modelling*, 56:137–157, 2018.

[35] T.D. Van Golf-Racht, editor. *fundamentals of fractured reservoir engineering*, volume 12 of *Developments in Petroleum Science*. Elsevier, 1982.

[36] Faisal Awad Aljuboori, Jang Hyun Lee, Khaled A Elraies, and Karl D Stephen. Effect of fracture characteristics on history matching in the Qamchuqa reservoir: a case study from Iraq. *Carbonates and Evaporites*, 35(3):87, 2020.